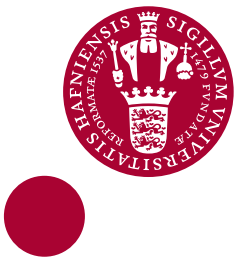

Quorum sensing determines the choice of antiphage defense strategy in Vibrio anguillarum

Tan, Demeng; Svenningsen, Sine Lo; Middelboe, Mathias

Published in:
mBio

DOI:
10.1128/mBio.00627-15

Publication date:
2015

Document version
Publisher's PDF, also known as Version of record

RESEARCH ARTICLE

Quorum Sensing Determines the Choice of Antiphage Defense Strategy in *Vibrio anguillarum*

Demeng Tan,[a] Sine Lo Svenningsen,[b] Mathias Middelboe[a]

Marine Biological Section, Department of Biology, University of Copenhagen, Copenhagen, Denmark[a]; Section for Biomolecular Sciences, Department of Biology, University of Copenhagen, Copenhagen, Denmark[b]

ABSTRACT **Selection for phage resistance is a key driver of bacterial diversity and evolution, and phage-host interactions may therefore have strong influence on the genetic and functional dynamics of bacterial communities. In this study, we found that an important, but so far largely overlooked, determinant of the outcome of phage-bacterial encounters in the fish pathogen *Vibrio anguillarum* is bacterial cell-cell communication, known as quorum sensing. Specifically, *V. anguillarum* PF430-3 cells locked in the low-cell-density state (Δ*vanT* mutant) express high levels of the phage receptor OmpK, resulting in a high susceptibility to phage KVP40, but achieve protection from infection by enhanced biofilm formation. By contrast, cells locked in the high-cell-density state (Δ*van*O mutant) are almost completely unsusceptible due to quorum-sensing-mediated downregulation of OmpK expression. The phenotypes of the two quorum-sensing mutant strains are accurately reflected in the behavior of wild-type *V. anguillarum*, which (i) displays increased OmpK expression in aggregated cells compared to free-living variants in the same culture, (ii) displays a clear inverse correlation between *ompK* mRNA levels and the concentration of *N*-acylhomoserine lactone quorum-sensing signals in the culture medium, and (iii) survives mainly by one of these two defense mechanisms, rather than by genetic mutation to phage resistance. Taken together, our results demonstrate that *V. anguillarum* employs quorum-sensing information to choose between two complementary antiphage defense strategies. Further, the prevalence of nonmutational defense mechanisms in strain PF430-3 suggests highly flexible adaptations to KVP40 phage infection pressure, possibly allowing the long-term coexistence of phage and host.**

IMPORTANCE **Comprehensive knowledge on bacterial antiphage strategies and their regulation is essential for understanding the role of phages as drivers of bacterial evolution and diversity. In an applied context, development of successful phage-based control of bacterial pathogens also requires detailed understanding of the mechanisms of phage protection in pathogenic bacteria. Here, we demonstrate for the first time the presence of quorum-sensing-regulated phage defense mechanisms in the fish pathogen *Vibrio anguillarum* and provide evidence that quorum-sensing regulation allows *V. anguillarum* to alternate between different phage protection mechanisms depending on population cell density. Further, our results demonstrate the prevalence of nonmutational defense mechanisms in the investigated *V. anguillarum* strain, which allow flexible adaptations to a dynamic phage infection pressure.**

Received 17 April 2015 **Accepted** 22 May 2015 **Published** 16 June 2015

Citation Tan D, Svenningsen SL, Middelboe M. 2015. Quorum sensing determines the choice of antiphage defense strategy in *Vibrio anguillarum*. mBio 6(3):e00627-15. doi: 10.1128/mBio.00627-15.

Editor Bonnie Bassler, Princeton University

Address correspondence to Mathias Middelboe, mmiddelboe@bio.ku.dk.

Vibrio anguillarum is a marine pathogenic bacterium which causes vibriosis in numerous fish and shellfish species, leading to high mortalities and economic losses in aquaculture worldwide (1). The use of bacteriophages to control bacterial infections in aquaculture has gained increased attention in the past few years, and successful application of phages to reduce vibriosis-related mortality has been demonstrated (2). Development of a phage-based treatment is, however, challenged by the wide variety of antiphage defense strategies observed in bacterial hosts (3). There is clear evidence that genetic mutation, normally causing disruption or modification of phage receptors in the host membrane, plays an important role in preventing phage infection in some cases (4–8). Such genetic changes may impose a fitness cost on the host cell as disruption of phage receptors can reduce the uptake of certain substrates (9–11). Alternative defense mechanisms which do not involve mutational changes have been described and also play a role in *V. anguillarum* (12). Aggregate formation and production of exopolysaccharides were suggested to provide protection against infection in *V. anguillarum* strain PF430-3 (7, 12). Recently, a more flexible protection mechanism was discovered in *Escherichia coli*, involving a temporary downregulation of phage receptor production in response to *N*-acyl-L-homoserine lactone (AHL) cell-cell signaling molecules (13). This mechanism is controlled by quorum sensing (QS), i.e., the ability of bacteria to regulate gene expression according to population density via the production and subsequent detection of extracellular signaling molecules (14).

Little is still known about the mechanisms of phage protection

in natural *Vibrio* communities. The universal outer membrane protein K (OmpK) has previously been shown to be the infection site for vibriophage KVP40, which infects more than eight *Vibrio* species, including *V. anguillarum*, *V. parahaemolyticus*, *V. harveyi*, and *V. cholerae* (15, 16). Mutations in this protein have been reported in *V. parahaemolyticus* R4000 upon exposure to KVP40 (15) but were not detected in KVP40-amended cultures of *V. anguillarum* PF430-3 (7, 12). Thus, other mechanisms for preventing infection by KVP40 in the *Vibrio* community may also be prevalent.

AHL-mediated QS circuits have been identified in many *Vibrio* species, including *V. anguillarum* (14, 17, 18). *V. anguillarum* controls QS-regulated genes via the transcription factor VanT, which is activated in response to extracellular signaling molecules (19, 20). At low autoinducer concentrations (i.e., low cell density), the response regulator VanO becomes activated by phosphorylation and represses the expression of VanT. At high cell densities, autoinducer concentrations increase and bind to membrane-bound receptors (19, 20). At a certain threshold concentration, VanO is dephosphorylated and VanT expression is induced, allowing gene regulation within the QS regulon (19, 20). Several *N*-acylhomoserine lactone autoinducers have been identified in stationary-phase *V. anguillarum* spent culture supernatant (21).

As densities of bacterial populations vary from sparsely populated environments to highly dense populations in nutrient-rich environments, and phages require a bacterial host in order to multiply, phage predation pressure is not constant and may be expected to correlate with the density of the bacterial host population, among other factors. Thus, bacteria could potentially benefit from altering their antiphage strategies depending on the perceived population density, thereby minimizing the metabolic burden often associated with resistance by genetic mutation (3, 9, 22, 23).

In this study, we identified a potent antiphage defense mechanism in *V. anguillarum* and showed that different antiphage strategies prevail at different population densities. Under high-cell-density conditions, QS-mediated downregulation of the OmpK receptor reduced phage adsorption and rendered individual cells almost unsusceptible to phage infection. Under low-cell-density conditions, on the other hand, OmpK expression was unaffected by QS and the individual cells were fully susceptible to infection. However, under these conditions, we have shown in a previous study that aggregation of the cells prevents phage from reaching the OmpK receptor (7, 12). In neither case was phage protection associated with *ompK* mutation. Overall, the study shows that QS controls the choice of antiphage defense strategy in the examined *V. anguillarum* strain PF430-3, suggesting the presence of dynamic, temporary adaptations to phage infection pressure, while still securing the ability to produce a functional OmpK receptor. In a phage therapy context, these results are highly relevant, as a combination of phage-based and anti-QS targeted treatments could enhance the efficiency of phage control of vibriosis.

RESULTS

We have recently demonstrated that addition of phage KVP40 to *V. anguillarum* strain PF430-3 resulted in increased cell aggregation and biofilm formation, which provided protection against phage infection (7, 12). However, at high cell densities, detachment of cells from aggregates into free-living variants was observed, which coexisted with phages (12), suggesting that alternative defense mechanisms also played a role under these conditions. Isolation and subsequent reculturing of these free-living cells in the absence of KVP40 showed that the recultured cells had regained sensitivity to phage KVP40 (7), suggesting that the initial protection was caused not by mutational changes but rather by a temporary protection mechanism. To test if an extracellular factor might be involved in the regulation of the phage-induced aggregation phenotype, we examined the effect of adding cell-free spent culture fluid from high-cell-density cultures of strain PF430-3 to freshly inoculated cultures of the same strain in the presence or absence of phage KVP40 by phase-contrast microscopy (Fig. 1, left panels). Intriguingly, the phage-induced aggregation phenotype of PF430-3 was completely inhibited by the presence of the cell-free spent culture fluid, suggesting that an extracellular factor(s), possibly a QS signaling molecule, is involved in the regulation of phage defense in *V. anguillarum* PF430-3.

Synthetic AHL-induced downregulation of phage production. *V. anguillarum* has been shown to produce at least three different AHL QS autoinducers, namely, *N*-(3-hydroxyhexanoyl) homoserine lactone (3-hydroxy-C_6-HSL), *N*-(3-oxodecanoyl) homoserine lactone, and *N*-hexanoylhomoserine lactone (C_6-HSL) (21). To further evaluate the role of QS in phage-host interactions in *V. anguillarum*, the effect of synthetic AHL addition on phage KVP40 production was quantified in strain PF430-3 (see Fig. S2 in the supplemental material). The results showed that the presence of synthetic AHL autoinducers in the medium reduced phage KVP40 production by 1.5- to 2-fold after 2 h relative to control cultures without AHL addition (see Fig. S2, squares). In parallel cultures grown without phage addition, cell growth was unaffected by AHL addition (see Fig. S2, circles).

KVP40 efficiency of plating on QS mutants of PF430-3. In order to examine the effects of QS on the interaction between phage KVP40 and *V. anguillarum* PF430-3, two otherwise isogenic QS mutants were constructed which represent cell behavior at high (Δ*vanO*) or low (Δ*vanT*) cell densities, respectively. Since the phosphorylated VanO protein represses the QS regulator VanT at low cell densities, the Δ*vanO* mutant displays full expression of VanT at all densities and is therefore locked in a high-cell-density phenotype (19). By contrast, a Δ*vanT* mutant has lost the ability to regulate QS-associated functions and is therefore locked in a low-cell-density phenotype. Use of the two extreme QS phenotypes of Δ*vanT* and Δ*vanO* mutants in the current study allowed us to explore the role of QS-mediated phage protection in *V. anguillarum* PF430-3. We first tested the infectivity of phage KVP40 on the wild-type *V. anguillarum* PF430-3 strain and the Δ*vanT*, Δ*vanO*, Δ*ompK*, Δ*vanT* Δ*ompK*, and Δ*vanO* Δ*ompK* constructed mutants by examining the efficiency of plating (EOP; the number of plaques obtained on each host from a given phage input). Relative to the wild-type strain, the phage susceptibility of the Δ*vanT* mutant had increased by 53%, and the plaque morphology had changed from turbid to clear (see Fig. S3A in the supplemental material). Additionally, the Δ*vanO* mutant had become less susceptible to phage infection with a reduction of 37% relative to the wild type (see Fig. S3B). As expected, Δ*ompK*, Δ*vanT* Δ*ompK*, and Δ*vanO* Δ*ompK* mutants had all become resistant to KVP40, confirming that OmpK is the phage receptor (see Fig. S3A).

Phage-host interactions in liquid cultures. Further assessments of QS-mediated regulation of phage infectivity in 10-h-infection experiments with phage KVP40 and three hosts (wild-type, Δ*vanT*, and Δ*vanO* strains) showed strong effects of the

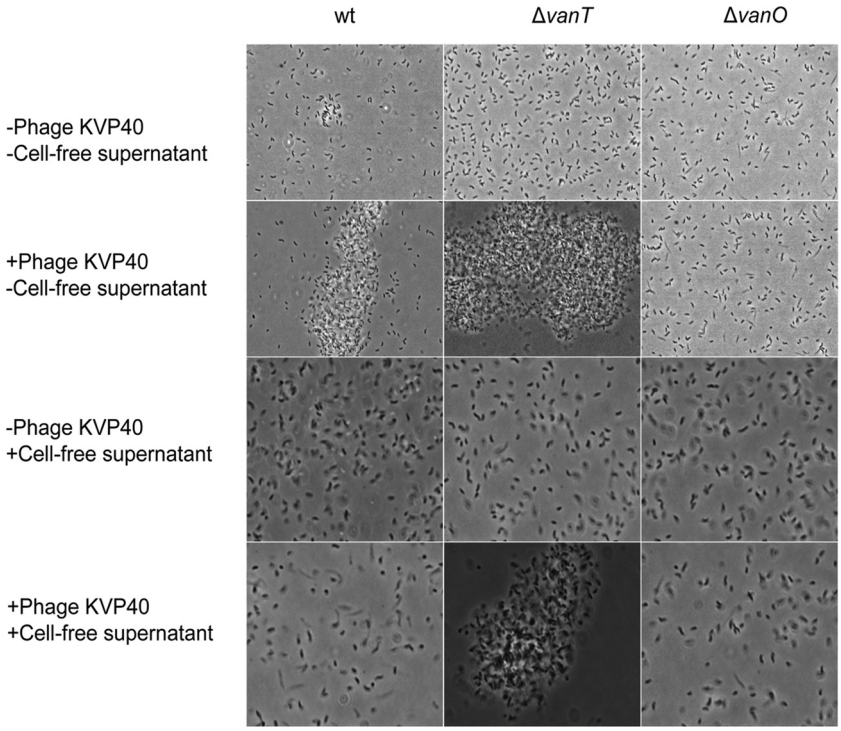

FIG 1 Visualization by phase-contrast microscopy of *V. anguillarum* strain PF430-3 (wild type [wt] and Δ*vanT* and Δ*vanO* mutants) in the presence or absence of phage KVP40 in either fresh marine broth or cell-free spent culture fluid obtained from a mid-log-phase culture of wild-type *V. anguillarum* PF430-3.

mutational changes on phage-host interactions. Phage KVP40 reduced cell density in the wild-type and Δ*vanT* cultures within the 10-h incubation by 60% and 75%, respectively, relative to the optical density (OD) of control cultures without phages, with significantly lower OD values in the Δ*vanT* culture than in the wild-type culture (0.62 and 0.88 after 10 h, respectively) (Fig. 2A). In the Δ*vanO* culture, on the other hand, OD was not significantly affected by phage addition (Fig. 2A). In accordance with these results, we observed rapid phage propagation in the wild-type and Δ*vanT* cultures where KVP40 abundance stabilized at ~10^{10} PFU ml^{-1}, whereas the phage production was ~100-fold lower in the Δ*vanO* culture (Fig. 2B). We note that the minimum OD values of 0.33 and 0.15 after 5 h in the phage-treated wild-type and Δ*vanT* cultures, respectively, were followed by a regrowth of cells during the remainder of the incubation (Fig. 2A), despite the abundance of KVP40 phage.

Aggregation of cells in the two QS mutants following phage KVP40 exposure was assessed by phase-contrast microscopy (Fig. 1, center and right panels; see also Fig. S1 in the supplemental material). Similar to the wild-type culture shown in Fig. 1, addition of phages led to increased aggregation in the Δ*vanT* mutant cultures. In fact, at 24 h most cells occurred in large aggregates in the Δ*vanT* mutant cultures, while a fraction of free-living cells was still detectable in the wild-type culture (Fig. 1; see also Fig. S1). In the Δ*vanO* cultures, on the other hand, phage addition did not result in formation of aggregates (Fig. 1; see also Fig. S1), suggesting that the QS pathway is involved in the regulation of the phage-induced aggregation phenotype. Furthermore, the addition of cell-free spent culture fluid, which prevented aggregation of the wild-type culture, did not prevent aggregation of the Δ*vanT* mutant cultures upon exposure to phage, suggesting that the inhibitory factor present in the cell-free culture fluid prevents aggregation via the QS pathway (Fig. 1). However, addition of the synthetic AHL autoinducers did not mimic the inhibitory effect of adding cell-free spent culture fluid on phage-induced aggregation in wild-type PF430-3 (data not shown).

Effects of phage KVP40 and QS on biofilm formation. Based on the indications of phage-driven stimulation of biofilm formations in the short-term liquid culture experiments, a more systematic quantification of the effects of phage KVP40 on biofilm formation in the three strains was performed. In the control cultures without phages, the biofilm formation of the wild-type and Δ*vanT* strains increased for 5 days and then remained constant at an OD at 595 nm (OD_{595}) of 1.5 to 1.75, as measured by crystal violet staining of the biofilm. In the Δ*vanO* cultures, the biofilm developed at a lower rate but reached the same endpoint as the other strains after 8 days (see Fig. S4A in the supplemental material). Pretreatment of the cultures with phage KVP40 enhanced biofilm formation in all 3 strains. The OD_{595} in wild-type and Δ*vanT* cultures reached values of 2.8 after 3 days, whereas OD_{595} in the KVP40-treated Δ*vanO* cultures increased gradually during the incubation to a maximum of 2.2 after 8 days (see Fig. S4A). Phage concentration in the liquid above the biofilm increased rapidly and stabilized around 10^9 PFU ml^{-1} in both wild-type and Δ*vanT* cultures after 1 day. In the Δ*vanO* + KVP40 cultures, phage concentration increased at a slower pace until day 3, where it also stabilized at ~10^9 PFU ml^{-1} (see Fig. S4B).

Together, the results from these experiments demonstrate a reduced susceptibility to phage KVP40 in the Δ*vanO* mutant despite the fact that this mutant aggregates less and forms biofilm more slowly than the wild type, suggesting that *V. anguillarum* PF430-3 may obtain protection against KVP40 via a separate

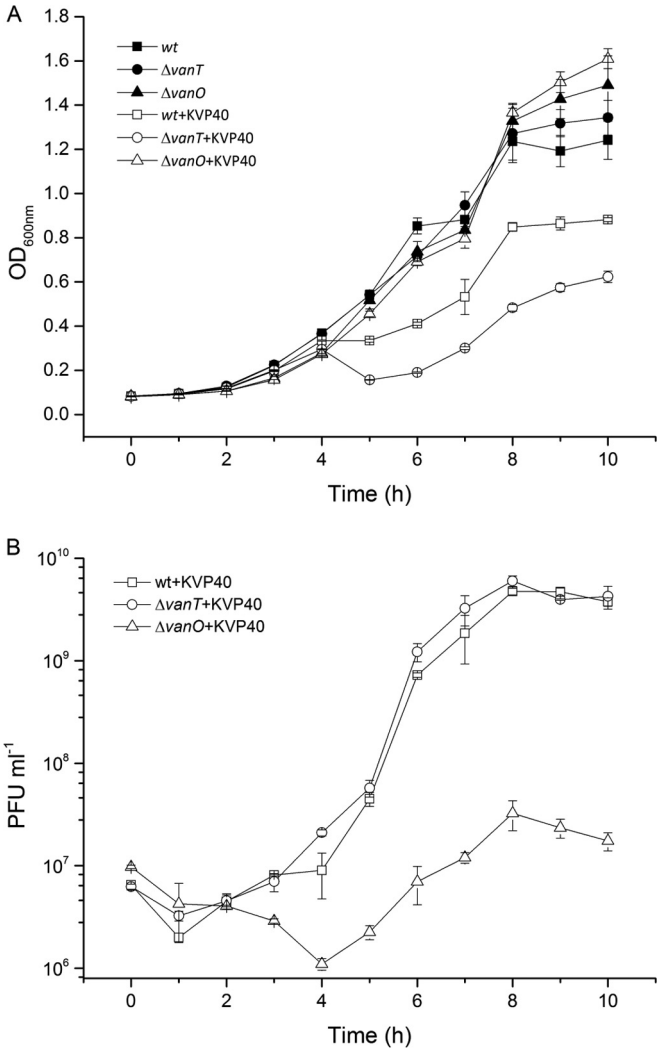

FIG 2 (A) Optical densities (OD_{600}) of cultures of *V. anguillarum* wild-type (wt) and QS mutant (Δ*vanT* and Δ*vanO*) strains in the presence or absence of phage KVP40 at an API of 1 were measured at 1-h intervals over a 10-h period of incubation. (B) Corresponding abundances of PFU per milliliter were quantified by plaque assay over a 10-h period of incubation in wild-type + KVP40, Δ*vanT* + KVP40, and Δ*vanO* + KVP40 cultures, respectively. Error bars represent standard deviations from all experiments carried out in duplicate.

mechanism in the high-cell-density QS mode mimicked by the Δ*vanO* mutant.

Phage adsorption rate. To address the question of how Δ*vanO* mutant cells reduce their susceptibility to KVP40, we first measured the rate of adsorption of KVP40 to the wild-type and QS mutant host cells. The adsorption rates of wild-type, Δ*vanT*, and Δ*vanO* strains were calculated as $6.7 \times 10^{-10} \pm 8.49 \times 10^{-11}$ ml^{-1} min^{-1}, $8.1 \times 10^{-10} \pm 9.2 \times 10^{-11}$ ml^{-1} min^{-1}, and $3.8 \times 10^{-10} \pm 1.4 \times 10^{-11}$ ml^{-1} min^{-1}, respectively. Thus, the rate of adsorption of phage KVP40 to the Δ*vanO* strain was significantly lower than that observed for the wild-type and Δ*vanT* strains.

***ompK* expression in cultures of wild-type and QS mutant cells.** To further examine the mechanism underlying the differences in adsorption rates among wild-type and QS mutant (Δ*vanT* and Δ*vanO*) strains and to link these differences to QS regulation, we quantified the expression of phage KVP40 receptor *ompK* in 9 different cultures (wild type, Δ*vanT*, Δ*vanO*, wild type + KVP40, Δ*vanT* + KVP40, Δ*vanO* + KVP40, Δ*ompK*, Δ*vanT* Δ*ompK*, and Δ*vanO* Δ*ompK*) by quantitative real-time PCR (qPCR). The relative *ompK* expression levels of wild-type and Δ*vanT* strains were approximately 4 times higher than the relative *ompK* expression in the Δ*vanO* strain, suggesting a downregulation of *ompK* when the cells are locked in the regulatory state mimicking high cell densities (Fig. 3A). Purification and separation of outer membrane proteins (OMPs) by SDS-PAGE (Fig. 3B) using three *ompK* mutants (Δ*ompK*, Δ*vanT* Δ*ompK*, and Δ*vanO* Δ*ompK* strains) as negative controls confirmed the presence of the OmpK receptor (26 kDa) in wild-type and Δ*vanT* strains and the QS-mediated OmpK receptor downregulation in the Δ*vanO* strain (15). In agreement with the gene expression data, OmpK appeared to be slightly more abundant in the Δ*vanT* strain than in the wild-type strain. SDS-PAGE outer membrane protein analysis also demonstrated that outer membrane proteins other than OmpK, which potentially function as phage receptors, were downregulated in the Δ*vanO* QS mutant as well (Fig. 3B, OmpK, indicated by arrow).

***ompK* mRNA levels in the free-living and aggregated cell fractions.** We have shown above that the Δ*vanT* mutant displays increased aggregation and contains high levels of *ompK*, whereas the Δ*vanO* mutant displays very little aggregation but instead reduces its susceptibility to phage KVP40 by expressing low levels of OmpK. Next, we verified whether these two phenotypes are also correlated in the wild-type PF430-3 strain. We fractionated cultures (wild type + KVP40, Δ*vanT* + KVP40, and Δ*vanO* + KVP40) into a free-living and an aggregate fraction by centrifugation and compared relative *ompK* mRNA levels in the two fractions using qPCR (Fig. 4). The analysis revealed that *ompK* gene expression varied significantly between aggregated and free-living cells in the wild-type strain, with approximately 2-fold-higher *ompK* mRNA levels in the bacteria located in aggregates than in the fraction containing free-living cells (Fig. 4). Moreover, it should be noted that the applied centrifugation procedure does not result in complete separation of the aggregates from the free-living cells; hence, the difference in *ompK* mRNA levels between the two fractions is likely underestimated. Interestingly, *ompK* mRNA levels were also higher in the aggregated fraction of the Δ*vanO* mutant cells than in the corresponding free-living fraction, although the *ompK* levels in both fractions were still much reduced compared to the wild-type or Δ*vanT* culture. Thus, even in the absence of a functional QS pathway, free-living cells express less *ompK* mRNA than do aggregated cells, which could either reflect the existence of a redundant VanO-independent regulatory mechanism or simply reflect a phage-mediated enrichment of cells with low *ompK* mRNA expression among the surviving free-living cells. Unfortunately, we were unable to collect free-living cells from Δ*vanT* cultures grown in the presence of phage, as any free-living cells were lysed by the phage and the remaining cells were all aggregated. However, in agreement with the data shown in Fig. 3A (*ompK* mRNA levels in the presence of phage KVP40), *ompK* mRNA levels were upregulated in the Δ*vanT* aggregates even compared to the wild-type aggregated fraction.

Temporal changes in *ompK* expression and AHL production in wild-type *V. anguillarum* PF430-3. In order to determine whether *ompK* expression was in fact repressed by a cell-density-

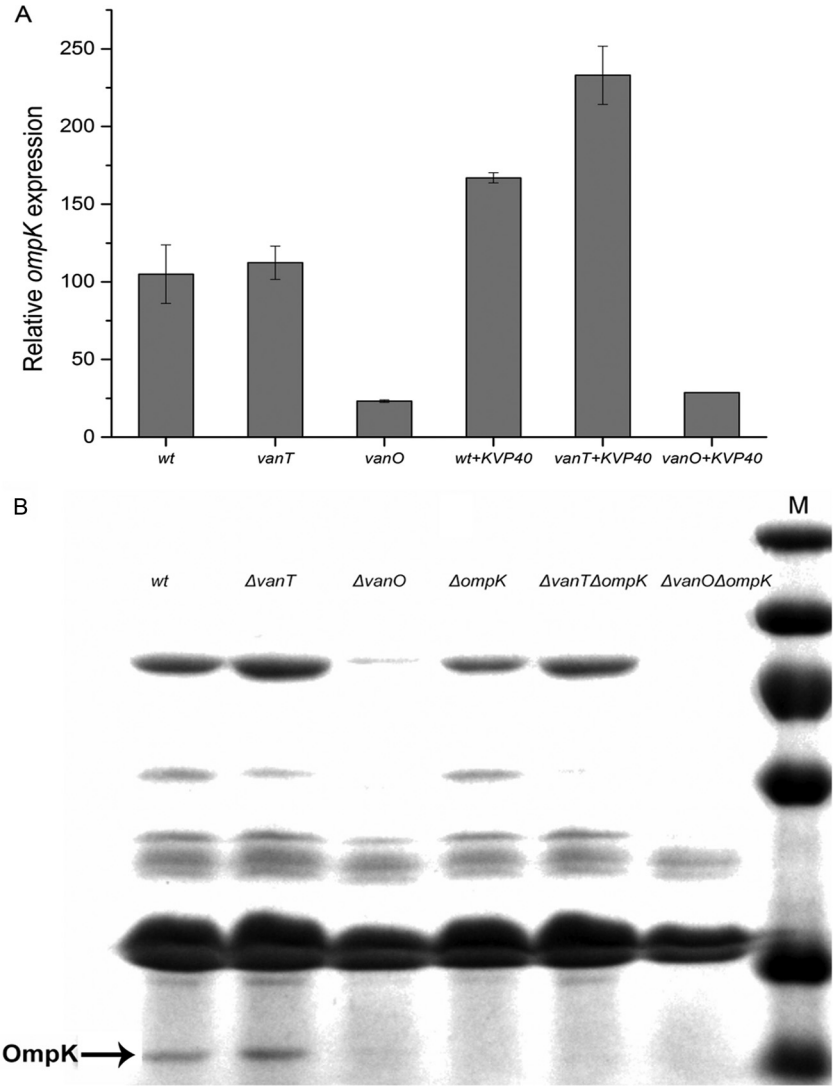

FIG 3 (A) *ompK* gene expression of wild type (wt) and QS mutants (Δ*vanT* and Δ*vanO*) in the presence or absence of phage KVP40. (B) SDS-PAGE analysis of the outer membrane protein K (OmpK) with Coomassie blue staining. Lane M, protein markers; lanes 1 to 6, wild-type, Δ*vanT*, Δ*vanO*, Δ*ompK*, Δ*ompK* Δ*vanT*, and Δ*ompK* Δ*vanO* strains, respectively. Phage receptor *ompK* mRNA transcript levels were quantified by real-time PCR. "Relative gene expression" corresponds to the level of *ompK* mRNA after normalization to the level of *recA* mRNA in the same sample. Error bars represent standard deviations (duplicate samples).

dependent factor secreted by the *V. anguillarum* PF430-3 wild-type strain, simultaneous measurements of *ompK* expression and extracellular AHL levels were performed during growth of the wild-type strain in batch culture in the absence of phages. Interestingly, phage receptor *ompK* expression and AHL levels were significantly negatively correlated ($r = 0.811$) during the first 12 h. Thus, in accordance with the previous experiment, *ompK* expression was 3 to 4 times higher at the low cell density around 2 h than at the high cell density at 6 h (Fig. 5). AHL production reached a maximum at 6 h and decreased after 8 h, concomitantly with an increase in *ompK* expression. After 16 h, a sharp decline in *ompK* expression was observed.

Examination of potential fitness costs in Δ*ompK* mutants. Throughout our studies of the interaction of phage KVP40 with *V. anguillarum* strain PF430-3, we did not once observe a single case of resistance to phage KVP40 infection due to mutation of *ompK*. By contrast, cells that survived exposure to phage KVP40 always multiplied to produce offspring that had regained phage sensitivity (7, 12). Therefore, we suggest that the sensitivity to phage KVP40 was related to regulation of phenotypic traits rather than genetic mutation. The physiological role of OmpK is not known, but Biolog GN2 physiological fingerprints of the wild-type strain and the Δ*ompK* mutant showed that the Δ*ompK* mutant lost the ability to utilize glucose-1-phosphate, glucose-6-phosphate, *cis*-aconitic acid, L-alaninamide, and L-alanine as growth substrates, suggesting that indeed OmpK may play an important role for *V. anguillarum* metabolism (see Fig. S5 in the supplemental material). We were, however, unable to detect a change in the relative abundance of the Δ*ompK* mutant compared to wild type after 8 h of growth in mixed culture. Thus, loss of the OmpK receptor does not directly affect the competitive ability of strain PF430-3 under our experimental conditions (see Fig. S6).

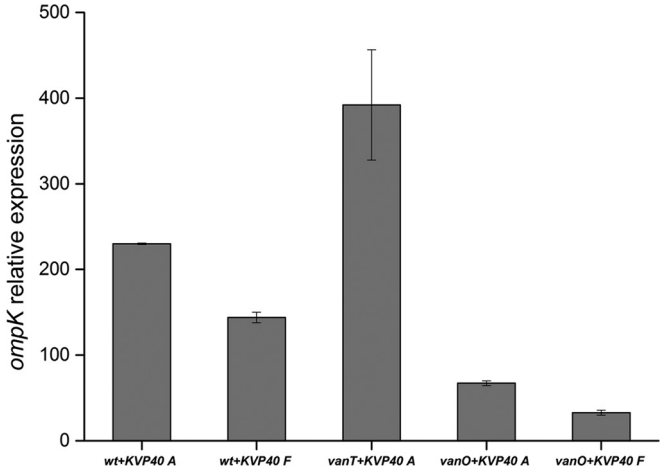

FIG 4 Fractionation experiment. For bacterial aggregates (A), samples were harvested at 1,000 × *g* for 10 min. For free-living bacteria (F), samples were harvested at 10,000 × *g* for 10 min. Phage receptor *ompK* mRNA transcript levels were quantified by real-time PCR. Relative gene expression was normalized against the gene expression level of *recA*. Error bars represent standard deviations (duplicate samples). wt, wild type.

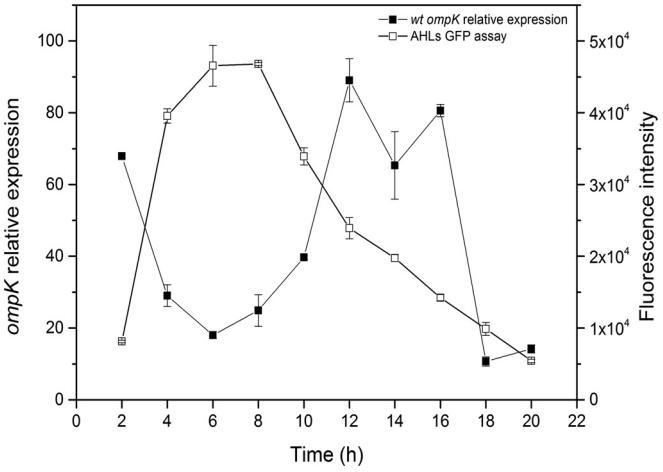

FIG 5 AHL assay and *ompK* expression quantification in the wild-type (wt) strain over time. Aliquots of cultures were withdrawn every 2 h during growth for measurement of AHL production and *ompK* gene expression by RT-PCR as described in the legend to Fig. 3. Error bars represent standard deviations (duplicate samples).

DISCUSSION

Given the recent findings that bacteria may employ QS to reduce phage receptor expression under conditions of high infection risk (13), we aimed at exploring the role of QS in regulating susceptibility to the broad-host-range phage KVP40 in *V. anguillarum* strain PF430-3 through downregulation of the phage receptor OmpK. The reduced susceptibility to phage KVP40 in *V. anguillarum* strain PF430-3 after addition of cell-free supernatant or synthetic AHLs provided the first indications of a QS-regulated mechanism of phage protection. This was further supported by our subsequent studies of phage susceptibility in the two constructed *V. anguillarum* QS mutants, the Δ*vanT* and Δ*vanO* strains. These results showed that phage susceptibility and adsorption were reduced in the Δ*vanO* strain and enhanced in the Δ*vanT* strain relative to the wild type, directly confirming that QS played a key role in the protection against KVP40 infection. The >100-fold-higher phage production and 3-fold-lower bacterial density in cultures of the Δ*vanT* strain relative to the Δ*vanO* strain after phage addition thus emphasized that QS signaling in the high-cell-density phenotype mediated an efficient protection against phage infection.

Measurements of the *ompK* expression further resolved the underlying mechanisms of QS-mediated phage protection. Thus, the significant (4-fold) reduction in *ompK* expression in the Δ*vanO* strain and the verification that an OmpK receptor-deficient mutant (the Δ*ompK* strain) was resistant to phage KVP40 provided direct evidence for QS-mediated downregulation of *ompK* expression as an important mechanism for protection against phage infection in *V. anguillarum*.

Interestingly, our results also showed that downregulation of *ompK* expression was not the only QS-regulated phage defense mechanism in the investigated *V. anguillarum* strain. Cell aggregation and formation of a biofilm in response to phage addition in the wild-type strain suggested that the transformation from a free-living life form to growth in a biofilm was also a mechanism of protection against phage infection, as also supported by a previous study (12). The exact mechanism by which phages induce cell aggregation, however, remains to be discovered. While the production of extracellular polymers by the host to create a physical barrier against phage infection has been suggested previously (3, 24), the current results suggest that this mechanism is QS controlled in *V. anguillarum*. Addition of phage KVP40 strongly stimulated cell aggregation and biofilm formation in the wild type and low-cell-density mutant (Δ*vanT*), whereas no aggregation was observed in the high-cell-density mutant (Δ*vanO*). Hence, the data suggest that cell aggregation and biofilm formation are an important phage defense mechanism at low cell densities where QS regulation of *ompK* expression is inefficient. Consequently, we show that *V. anguillarum* PF430-3 alternates between these two types of phage defense mechanisms and that QS regulates the choice of strategy by upregulating one mechanism (removal of OmpK receptor) while downregulating another mechanism (cell aggregation) at high cell densities. Whether the overall reduction in OmpK receptors under high-cell-density conditions results in a general decrease in the number of receptors per cell in the population, thus reducing the encounter rate between phages and OmpK receptors, and/or if OmpK downregulation generates a fraction of cells completely without receptors (i.e., resistant cells), is not known. However, the presence of turbid plaques in the Δ*vanO* mutant upon exposure to KVP40 in spot assays indicated that some of the cells were, in fact, temporarily fully resistant to the phage. The presence of two distinct phage defense mechanisms in wild-type cells was confirmed by the observation that *ompK* expression was reduced in free-living cells relative to cells embedded in aggregates. Together with the significant negative correlation between extracellular AHL concentration and *ompK* expression during growth of the wild-type strain in batch cultures, this demonstrated the dynamic nature of phage defense and emphasized that the obtained results were not restricted to the extreme phenotypes of the QS mutants. Interestingly, *ompK* expression was in fact enhanced in phage-amended wild-type and Δ*vanT* cultures relative to control cultures without phages. OmpK is a porin-like protein which has been suggested to be involved in bile salt resis-

tance, as well as iron acquisition (25). We show here that OmpK also plays a role in the ability of *V. anguillarum* to use glucose-1-phosphate, glucose-6-phosphate, *cis*-aconitic acid, L-alaninamide, and L-alanine as growth substrates. We speculate therefore that upregulation of *ompK* in aggregated cells may be an adaptation to stimulate nutrient uptake in an aggregate environment where supply of specific nutrients may be limited or for enhancing the bile salt resistance of the cell aggregates inside the host. However, in the short-term competition experiment that we carried out, the Δ*ompK* mutant was able to reach the same density as the wild-type strain in a mixed culture. Further studies are needed to determine the physiological role(s) of OmpK and hence the cost of its repression or loss.

We note that in the wild-type cultures of *V. anguillarum* PF430-3, AHLs accumulate as the culture grows to high cell densities, but they largely disappear later in stationary phase (Fig. 5). This phenomenon has been observed previously in cultures of *Yersinia pseudotuberculosis* and *Pseudomonas aeruginosa*, grown in LB medium, and was found to be caused by pH-dependent lactonolysis (26). We found, however, that the pH of the marine broth (MB) cultures used here remained stable around 7.6 for at least 13 h (data not shown). Alternative explanations for the disappearance of the AHLs in stationary phase are the possible production of an AHL lactonase enzyme as reported in *Bacillus* spp. (27) or the uptake of AHLs for use as a source of energy, carbon, and nitrogen, as reported for *Variovorax paradoxus* (28). Additional studies are required to determine the mechanism responsible for AHL removal in *V. anguillarum* strain PF430-3.

One surprising observation from the current study was that QS reduced biofilm formation (see Fig. S4 in the supplemental material). Biofilm formation is in many bacterial pathogens found to be upregulated by QS and stimulated at high cell density, promoting virulence (29). This has also been observed in *V. anguillarum* (strain NB10), where a low-cell-density mutant (Δ*vanT* strain) showed significantly lower biofilm formation than the wild-type strain (30). The reason for this contrasting effect of QS on biofilm formation in PF430-3 is not clear. *V. anguillarum* strain NB10 showed limited susceptibility to phage KVP40 and produced turbid plaques (data not shown), suggesting that KVP40 is not an important predator on that strain; hence, other antiphage strategies may be favored. VanT expression is known to regulate physiological responses required for survival and stress response (19), and in the investigated strain PF430-3, this seems to include shifting from aggregation to *ompK* downregulation in response to increased cell density. In addition, since total protease activity correlates with VanT expression in *V. anguillarum* strain NB10 (30), it may be speculated that at high cell densities, when VanT is fully expressed, VanT activates protease activity to promote the release of cells from aggregates, in a manner similar to the action of the VanT homologue HapR in *V. cholerae*, where QS also downregulates biofilm formation (31, 32). By QS-mediated *ompK* gene regulation, aggregate-associated bacteria may thus have evolved a mechanism of detaching a subpopulation of free-living cells with reduced phage susceptibility which can survive in phage-dense environments, thus allowing further spreading of vibriosis infections. In any case, the results support previous indications of large differences in phage defense strategies among different strains of *V. anguillarum* (12) and emphasize the need for further exploring whether the mechanisms described here are a general phenomenon in bacteria or are limited to a subset of *V. anguillarum* strains.

Phages are known to be key drivers of bacterial evolution by selecting for phage-resistant mutants, and it has been proposed that phage-host interactions lead to either an arms race dynamic of antagonistic host and phage coevolution or a fluctuating selection dynamic involving frequency-dependent selection for rare host and phage genotypes (33, 34). In this study, however, we found evidence for an alternative to these scenarios, as the defense mechanisms identified do not involve mutational changes or complete elimination of phage-susceptible host cells. The described antiphage mechanisms in *V. anguillarum* thus represent more flexible adaptations to dynamic changes in phage and host densities, adding to the complexity of phage-host coevolutionary interactions and phage-driven genetic and phenotypic changes in bacterial populations. Since mutational changes often result in a loss of fitness for the host (9, 10), the mechanisms described here represent a potential fitness advantage for the host. It may be speculated that the development of this temporary protection mechanism in *V. anguillarum* PF430-3 is related to the fact that the OmpK receptor is widely conserved among *Vibrio* and *Photobacterium* species and thus probably executes an important function(s) in the cell. It is likely, therefore, that mutations in *ompK* could have significantly negative effects on host fitness in natural habitats, in which case development of alternative phage defense strategies that leave the *ompK* gene intact would be of strong selective advantage. Further studies are needed, however, to confirm this hypothesis.

Successful application of phage therapy in the treatment of vibriosis requires detailed knowledge of the phage-host interactions and the regulation of antiphage strategies in *Vibrio*. Our results add to the suite of known phage defense mechanisms and their regulation in marine bacteria and further emphasize that the complexity of phage-host interactions poses a challenge for future use of phages in disease control. On the other hand, the evidence that QS regulates phage receptor expression may potentially be used actively by quenching QS signaling, hence preventing receptor downregulation. In support of that, QS inhibitors have been shown to impede expression of virulence factors (35), and recently, the addition of modified T7 phages producing quorum-quenching enzymes has resulted in inhibition of biofilm formation, suggesting that the use of QS inhibitors may be a promising strategy in future antimicrobial therapy (36).

MATERIALS AND METHODS

Bacterial strains and bacteriophages. The bacterial strain *V. anguillarum* PF430-3 was originally isolated from salmonid aquaculture in Chile (37), and phage KVP40, which infects PF430-3, is a broad-host-range phage originally isolated from Japan (38) (see Table S1 in the supplemental material). Basic characterization of phage KVP40 and its interactions with PF430-3 has been provided recently (7). All the constructed mutant strains derived from the *V. anguillarum* PF430-3 wild-type strain and the plasmids used in this study are listed in Table S1 in the supplemental material. *E. coli* S17-1 (λ*pir*) was used as the donor strain for transfer of plasmid DNA into *V. anguillarum* PF430-3 by conjugation (30, 39). Antibiotics were used at the following concentrations: 100 $\mu g \cdot ml^{-1}$ ampicillin, 25 $\mu g \cdot ml^{-1}$ chloramphenicol (for *E. coli*), and 5 $\mu g \cdot ml^{-1}$ chloramphenicol (for *V. anguillarum*) (30, 39).

DNA manipulation and mutant construction. For mutant constructions, in-frame deletions were made in the *vanT*, *vanO*, and *ompK* genes by allelic exchange as first described by Croxatto et al. (30) and Milton et al. (39). The upstream DNA sequence of the *vanT* gene was amplified from wild-type *V. anguillarum* PF430-3 by PCR using primers vT1 and vT2, which introduced a BglII site. The downstream DNA sequence of

vanT was amplified using primers vT3 and vT4, which introduced a SacI site. These two fragments, which contain a 15-nucleotide (nt) overlap of identical sequence, were used as the template for a second PCR using primers vT1 and vT4. The PCR product was digested with BglII and SacI and cloned into the BglII and SacI sites of pDM4, creating pDM4vanT. In-frame deletion of *vanT* in PF430-3 was confirmed by PCR using primers vT1 and vT4 and subsequent gel electrophoresis. To construct plasmid pDM4vanO and pDM4ompK, and *vanO* and *ompK* mutants, we used the same method described for *vanT* above. The primers are listed in Table S2 in the supplemental material.

Examination of fitness loss in the *ompK* mutant. In an attempt to search for potential functions of phage receptor OmpK and, hence, implications of its downregulation or loss, Biolog GN2 microplates (Biolog) containing 95 different carbon sources were used to test the ability of the wild-type strain and the Δ*ompK* mutant to use different substrates according to the manufacturer's instructions. Further, the potential reduction in competitive abilities of the Δ*ompK* mutant was examined in competition assays. Briefly, wild-type and Δ*ompK* bacterial cells were mixed in a ratio of 1:1 in sterilized seawater and then quantified over time. Subsamples were collected every 1 to 2 h for 8 h and diluted and plated on LB plates. Subsequently, 20 colonies were picked from each time point and identified as either wild type or Δ*ompK* mutant by PCR with primers 1340F and 1340R listed in Table S2 in the supplemental material.

Effects of cell-free supernatant enrichment on KVP40 phage infection. Cell-free supernatant from wild-type *V. anguillarum* PF430-3 cultures was prepared from a mid-log-phase culture of *V. anguillarum* PF430-3 in marine broth (MB), which was centrifuged (10,000 × *g* for 10 min), sterile filtered (0.2 μm; Millipore), and subsequently added to freshly inoculated cultures of wild-type, Δ*vanT*, and Δ*vanO* strains, with and without phage KVP40, for examination of the potential effects of *V. anguillarum* PF430-3-produced autoinducer molecules on the lytic effects of the phage KVP40. Images were obtained after 24 h of incubation.

Effects of synthetic AHLs on phage production in *V. anguillarum* PF430-3 wild type. Synthetic AHLs (obtained from Sigma and Nottingham University), *N*-hexanoylhomoserine lactone (C_6-HSL), *N*-(3-hydroxyhexanoyl)homoserine lactone (3-hydroxy-C_6-HSL), and *N*-(3-oxodecanoyl)-L-homoserine lactone (3-oxo-C_{10}-HSL) were added to *V. anguillarum* PF430-3 to examine their effects on phage susceptibility. Briefly, the AHLs were dissolved in acidified ethyl acetate (0.1% [vol/vol] acetic acid), mixed, and added to a glass test tube to a 10 μM final concentration and placed at room temperature (RT) for complete evaporation of the solvent, as described previously (13, 40). For the control cultures without AHLs, test tubes containing only ethyl acetate were prepared in parallel. Overnight cultures of wild-type cells were pelleted and resuspended, and aliquots of 100 μl of cell suspension were transferred to 5 ml of 3% NaCl buffer in tubes containing AHLs or the solvent control and incubated at 30°C for 1 h. The phage susceptibility assay was then initiated by addition of phage KVP40 at an average phage input (API) of 1. Parallel control cultures without phages were also established. Samples were collected every hour for 7 h for quantification of possible effects of AHL on cell growth in the absence of phage (CFU) and on phage production (PFU).

Phage-host interactions and effects on cell aggregation in wild type and QS mutants. The susceptibility of each strain (wild-type, Δ*vanT*, Δ*vanO*, Δ*ompK*, Δ*vanT* Δ*ompK*, and Δ*vanO* Δ*ompK* strains) to phage KVP40 was gauged by the efficiency of plating. Briefly, a fixed quantity of phage obtained from the same phage stock (KVP40) was mixed with identically grown bacterial cells of each genotype, and the PFU were quantified by plaque assay (41). The experiments were performed in duplicate.

The lytic potential of phage KVP40 against wild-type and QS mutant strains (Δ*vanT* and Δ*vanO*) was tested at an API of 1 in duplicate 100-ml liquid MB cultures and parallel control cultures without phage. The effect of phage-mediated lysis on host cell density was monitored by regular OD_{600} measurement over the 10-h incubation. Phage concentration was quantified by plaque assay periodically (41).

For visual inspection of cell densities and aggregate formation, additional aliquots were collected at 24 h and visualized by phase-contrast microscopy using an oil immersion objective (Olympus BX61). The images shown in Fig. 1 and in Fig. S1 in the supplemental material represent random fields on the microscope slide from the 24-h samples.

Effects of phage addition on biofilm formation in wild-type and QS mutant strains. Biofilm formation was monitored in wild-type, Δ*vanT*, and Δ*vanO* cultures following addition of phage KVP40 using methods described previously (42) with some modifications. Briefly, 13-ml polypropylene plastic tubes filled with 5 ml MB were inoculated with 100 μl of overnight bacterial inoculum and 100 μl of phage stock (10^8 CFU ml^{-1} and 10^6 PFU ml^{-1}; API of 0.01) and incubated without shaking along with parallel control cultures without phages. For each experiment, duplicate tubes were examined daily for quantification of phage abundance in the liquid phase (41) and biofilm biomass was quantified by crystal violet staining using a standard protocol (43). For biofilm quantification, the liquid was removed, and tubes were rinsed twice with artificial seawater (ASW; Sigma). The biofilm was stained with 0.4% crystal violet (Sigma) for 15 min, and the tubes were washed with tap water to remove excess stain. An aliquot (6 ml) of 33% acetic acid (Sigma) was added and left for 5 min to allow the stain to dissolve. The absorbance was measured as OD_{595}.

Bacteriophage adsorption rate. The rates of adsorption of phage KVP40 to wild-type, Δ*vanT*, and Δ*vanO* cells were determined by mixing phage KVP40 and exponentially growing host cultures at an API of 0.01 and incubating them at room temperature for 32 min with agitation. Aliquots were removed periodically and centrifuged at 18,000 × *g* at 4°C for 2 min, and the supernatants were immediately diluted to prevent additional adsorption. The unadsorbed phage particles were quantified by plaque assay (41).

Outer membrane protein K (OmpK) preparation and SDS-PAGE analysis. The outer membrane protein (OMP) preparation was made essentially according to the method of Wang et al. (44) with some modifications. Briefly, cells were pelleted from 25-ml overnight cultures of all the strains (wild type and Δ*vanT*, Δ*vanO*, Δ*ompK*, Δ*vanT* Δ*ompK*, and Δ*vanO* Δ*ompK* mutants), resuspended in 4.5 ml of water, and sonicated on ice (amplitude of 100, 3 min). To solubilize the cytoplasmic membranes, Sarkosyl (*N*-lauroylsarcosine) was added to a final concentration of 2% and incubated at room temperature for 30 min. To pellet the outer membranes, the mixture was ultracentrifuged (400,000 rpm for 1 h at 4°C; SW55 Ti rotor; Beckman). The pellet was washed with ice-cold water and ultracentrifuged again (400,000 rpm for 30 min at 4°C; SW55 Ti rotor; Beckman). The pellet was resuspended in 100 μl 100 mM Tris-HCl (pH 8) and 2% SDS buffer, and the proteins were separated on a 10% SDS-polyacrylamide gel and stained with Coomassie blue.

Fractionation of *V. anguillarum* cultures in aggregate and free-living cell fractions. In order to examine *ompK* gene expression patterns in aggregates and free-living cells, respectively, cultures were fractionated by centrifugation and *ompK* expression was determined in the aggregate and nonaggregate fractions. Cultures of *V. anguillarum* wild type and QS mutants were grown in MB in the presence of phage KVP40 at an API of 1 at room temperature (RT) for 12 h, and the aggregates were collected by centrifugation (1,000 × *g*, 10 min). The supernatant was transferred to a new tube, and centrifugation was repeated. After the second round of centrifugation, the free-living cells in the supernatant were transferred to a new tube and collected by centrifugation at 10,000 × *g* for 10 min. Pellets of cell aggregates and free-living cells were collected and stored at −80°C for subsequent RNA extraction.

AHL signal levels in cultures of wild-type *V. anguillarum* PF430-3. An overnight culture of the wild-type strain was diluted in MB to a final OD_{600} of 0.04 and grown at 30°C for 20 h with agitation. Samples were taken every 2 h for determination of AHL production and for extraction of RNA for *ompK* mRNA quantification. AHL biosynthesis was assayed using the *E. coli* SP436 reporter strain (45). *E. coli* SP436 harbors a plasmid-borne fusion of the *V. fischeri* lux operon to *gfp* and responds to AHL by

expressing green fluorescent protein (GFP) as described previously (45). Briefly, 50 μl cell-free supernatant was mixed with 150 μl LB medium and 10 μl of an overnight culture of SP436 (100 μg · ml^{-1} ampicillin) and further incubated at 30°C for 5 h with agitation using a FLUOstar Omega microtiter plate reader (BMG Labtech) with a gain setting of 1,150.

RNA extraction and cDNA synthesis. For quantification of *ompK* expression in the wild-type and QS mutant strains (Δ*vanT* and Δ*vanO*), RNA was extracted from cells pelleted after a 9-h incubation in MB for the experiments shown in Fig. 5 or as described above for the experiments shown in Fig. 3 and 4. Total RNA was extracted using Trizol (Invitrogen) and chloroform extraction as described previously (46). Genomic DNA was removed by adding DNase I according to the manufacturer's protocol (Fermentas). RNA was stored at −80°C until further use.

Reverse transcription was performed with the Thermo Scientific Revert Aid first-strand cDNA synthesis kit as described by the manufacturer (Thermo). The first cDNA strand was obtained using random hexamer primers with 1,000 ng of DNase I-treated RNA. Control samples (without reverse transcriptase) were treated identically except that the reverse transcriptase enzyme was omitted.

RT-PCR gene expression quantification. The relative expression levels of *ompK* and *recA* (as the endogenous control) were determined by qPCR performed in a CFX96 real-time PCR (RT-PCR) detection system (Bio-Rad), using SsoAdvanced SYBR green supermix (Bio-Rad) and the gene-specific primers listed in Table S2 in the supplemental material (47). Quantitative PCR mixtures were set up in 25 μl containing 0.2 μM primers and SYBR green qPCR mix with the following program: 30 s at 95°C for denaturation followed by 40 cycles of 4 s at 95°C and 30 s at 55°C. Melting curve analysis was performed from 65°C to 95°C with an increment of 0.5°C for 5 s. The comparative threshold cycle (C_T) method was used for relative quantification of RNA (48).

SUPPLEMENTAL MATERIAL

Supplemental material for this article may be found at http://mbio.asm.org/lookup/suppl/doi:10.1128/mBio.00627-15/-/DCSupplemental.

Figure S1, PNG file, 2.3 MB.
Figure S2, TIF file, 0.9 MB.
Figure S3, TIF file, 2.1 MB.
Figure S4, TIF file, 1.1 MB.
Figure S5, TIF file, 0.7 MB.
Figure S6, TIF file, 0.8 MB.
Table S1, DOCX file, 0.01 MB.
Table S2, DOCX file, 0.01 MB.

ACKNOWLEDGMENTS

The study was supported by the Danish Council for Strategic Research (ProAqua project 12-132390) and the EU-IRSES-funded project AQUAPHAGE (269175).

We thank Debra Milton, Umeå University, for providing plasmid pDM4 and *E. coli* S1-17 and Pantelis Katharios, Hellenic Centre for Marine Research, for providing *V. anguillarum* PF430-3 and vibriophage KVP40. We are grateful to Nina Molin Høyland-Kroghsbo for many helpful discussions.

REFERENCES

1. **Frans I, Michiels CW, Bossier P, Willems KA, Lievens B, Rediers H.** 2011. *Vibrio anguillarum* as a fish pathogen: virulence factors, diagnosis and prevention. J Fish Dis **34:**643–661. http://dx.doi.org/10.1111/j.1365-2761.2011.01279.x.
2. **Vinod MG, Shivu MM, Umesha KR, Rajeeva BC, Krohne G, Karunasagar I, Karunasagar I.** 2006. Isolation of *Vibrio harveyi* bacteriophage with a potential for biocontrol of luminous vibriosis in hatchery environments. Aquaculture **255:**117–124. http://dx.doi.org/10.1016/j.aquaculture.2005.12.003.
3. **Labrie SJ, Samson JE, Moineau S.** 2010. Bacteriophage resistance mechanisms. Nat Rev Microbiol **8:**317–327. http://dx.doi.org/10.1038/nrmicro2315.
4. **Luria SE, Delbrück M.** 1943. Mutations of bacteria from virus sensitivity to virus resistance. Genetics **28:**491–511.
5. **Morona R, Klose M, Henning U.** 1984. Escherichia coli K-12 outer membrane protein (OmpA) as a bacteriophage receptor: analysis of mutant genes expressing altered proteins. J Bacteriol **159:**570–578.
6. **Bassford PJ, Jr., Diedrich DL, Schnaitman CL, Reeves P.** 1977. Outer membrane proteins of *Escherichia coli*. VI. Protein alteration in bacteriophage-resistant mutants. J Bacteriol **131:**608–622.
7. **Tan D, Gram L, Middelboe M.** 2014. Vibriophages and their interactions with the fish pathogen *Vibrio anguillarum*. Appl Environ Microbiol **80:**3128–3140. http://dx.doi.org/10.1128/AEM.03544-13.
8. **Guglielmotti DM, Reinheimer JA, Binetti AG, Giraffa G, Carminati D, Quiberoni A.** 2006. Characterization of spontaneous phage-resistant derivatives of *Lactobacillus delbrueckii* commercial strains. Int J Food Microbiol **111:**126–133. http://dx.doi.org/10.1016/j.ijfoodmicro.2006.04.035.
9. **Lenski RE.** 1988. Experimental studies of pleiotropy and epistasis in *Escherichia coli*. I. Variation in competitive fitness among mutants resistant to virus T4. Evolution **42:**425–432.
10. **Lenski RE, Levin BR.** 1985. Constraints on the coevolution of bacteria and virulent phage—a model, some experiments, and predictions for natural communities. Am Nat **125:**585–602. http://dx.doi.org/10.1086/284364.
11. **Szmelcman S, Hofnung M.** 1975. Maltose transport in *Escherichia coli* K-12: involvement of the bacteriophage lambda receptor. J Bacteriol **124:**112–118.
12. **Tan D, Dahl A, Middelboe M.** 24 April 2015. Vibriophages differentially influence biofilm formation by *Vibrio anguillarum* strains. Appl Environ Microbiol http://dx.doi.org/10.1128/AEM.00518-15.
13. **Høyland-Kroghsbo NM, Maerkedahl RB, Svenningsen SL.** 2013. A quorum-sensing-induced bacteriophage defense mechanism. mBio **4**(1):e00362-12. http://dx.doi.org/10.1128/mBio.00362-12.
14. **Miller MB, Bassler BL.** 2001. Quorum sensing in bacteria. Annu Rev Microbiol **55:**165–199. http://dx.doi.org/10.1146/annurev.micro.55.1.165.
15. **Inoue T, Matsuzaki S, Tanaka S.** 1995. A 26-kDa outer membrane protein, OmpK, common to *Vibrio* species is the receptor for a broad-host-range vibriophage, KVP40. FEMS Microbiol Lett **125:**101–105. http://dx.doi.org/10.1111/j.1574-6968.1995.tb07342.x.
16. **Inoue T, Matsuzaki S, Tanaka S.** 1995. Cloning and sequence analysis of *Vibrio parahaemolyticus* ompK gene encoding a 26-kDa outer membrane protein, OmpK, that serves as receptor for a broad-host-range vibriophage, KVP40. FEMS Microbiol Lett **134:**245–249.
17. **Bassler BL, Greenberg EP, Stevens AM.** 1997. Cross-species induction of luminescence in the quorum-sensing bacterium *Vibrio harveyi*. J Bacteriol **179:**4043–4045.
18. **Milton DL, Hardman A, Camara M, Chhabra SR, Bycroft BW, Stewart GS, Williams P.** 1997. Quorum sensing in *Vibrio anguillarum*: characterization of the *vanI*/*vanR* locus and identification of the autoinducer *N*-(3-oxodecanoyl)-L-homoserine lactone. J Bacteriol **179:**3004–3012.
19. **Weber B, Lindell K, El Qaidi S, Hjerde E, Willassen NP, Milton DL.** 2011. The phosphotransferase VanU represses expression of four *qrr* genes antagonizing VanO-mediated quorum-sensing regulation in *Vibrio anguillarum*. Microbiology **157:**3324–3339. http://dx.doi.org/10.1099/mic.0.051011-0.
20. **Croxatto A, Pride J, Hardman A, Williams P, Cámara M, Milton DL.** 2004. A distinctive dual-channel quorum-sensing system operates in *Vibrio anguillarum*. Mol Microbiol **52:**1677–1689. http://dx.doi.org/10.1111/j.1365-2958.2004.04083.x.
21. **Milton DL, Chalker VJ, Kirke D, Hardman A, Cámara M, Williams P.** 2001. The LuxM homologue VanM from *Vibrio anguillarum* directs the synthesis of *N*-(3-hydroxyhexanoyl)homoserine lactone and *N*-hexanoylhomoserine lactone. J Bacteriol **183:**3537–3547. http://dx.doi.org/10.1128/JB.183.12.3537-3547.2001.
22. **Lenski RE.** 1988. Experimental studies of pleiotropy and epistasis in *Escherichia coli*. II. Compensation for maladaptive effects associated with resistance to virus T4. Evolution **42:**433–440.
23. **Middelboe M, Holmfeldt K, Riemann L, Nybroe O, Haaber J.** 2009. Bacteriophages drive strain diversification in a marine *Flavobacterium*: implications for phage resistance and physiological properties. Environ Microbiol **11:**1971–1982. http://dx.doi.org/10.1111/j.1462-2920.2009.01920.x.
24. **Heilmann S, Sneppen K, Krishna S.** 2012. Coexistence of phage and bacteria on the boundary of self-organized refuges. Proc Natl Acad Sci U S A **109:**12828–12833. http://dx.doi.org/10.1073/pnas.1200771109.
25. **Hamod MA, Bhowmick PP, Shukur YN, Karunasagar I, Karunasagar I.**

2014. Iron shortage and bile salts play a major role in the expression of ompK gene in *Vibrio anguillarum*. Pol J Microbiol **63:**27–31.
26. **Yates EA, Philipp B, Buckley C, Atkinson S, Chhabra SR, Sockett RE, Goldner M, Dessaux Y, Cámara M, Smith H, Williams P.** 2002. *N*-Acylhomoserine lactones undergo lactonolysis in a pH-, temperature-, and acyl chain length-dependent manner during growth of *Yersinia pseudotuberculosis* and *Pseudomonas aeruginosa*. Infect Immun **70:**5635–5646. http://dx.doi.org/10.1128/IAI.70.10.5635-5646.2002.
27. **Dong YH, Gusti AR, Zhang Q, Xu JL, Zhang LH.** 2002. Identification of quorum-quenching *N*-acyl homoserine lactonases from *Bacillus* species. Appl Environ Microbiol **68:**1754–1759. http://dx.doi.org/10.1128/AEM.68.4.1754-1759.2002.
28. **Leadbetter JR, Greenberg EP.** 2000. Metabolism of acyl-homoserine lactone quorum-sensing signals by *Variovorax paradoxus*. J Bacteriol **182:**6921–6926. http://dx.doi.org/10.1128/JB.182.24.6921-6926.2000.
29. **Davies DG, Parsek MR, Pearson JP, Iglewski BH, Costerton JW, Greenberg EP.** 1998. The involvement of cell-to-cell signals in the development of a bacterial biofilm. Science **280:**295–298. http://dx.doi.org/10.1126/science.280.5361.295.
30. **Croxatto A, Chalker VJ, Lauritz J, Jass J, Hardman A, Williams P, Cámara M, Milton DL.** 2002. VanT, a homologue of *Vibrio harveyi* LuxR, regulates serine, metalloprotease, pigment, and biofilm production in *Vibrio anguillarum*. J Bacteriol **184:**1617–1629. http://dx.doi.org/10.1128/JB.184.6.1617-1629.2002.
31. **Jobling MG, Holmes RK.** 1997. Characterization of hapR, a positive regulator of the *Vibrio cholerae* HA/protease gene hap, and its identification as a functional homologue of the *Vibrio harveyi luxR* gene. Mol Microbiol **26:**1023–1034. http://dx.doi.org/10.1046/j.1365-2958.1997.6402011.x.
32. **Hammer BK, Bassler BL.** 2003. Quorum sensing controls biofilm formation in *Vibrio cholerae*. Mol Microbiol **50:**101–104. http://dx.doi.org/10.1046/j.1365-2958.2003.03688.x.
33. **Martiny JB, Riemann L, Marston MF, Middelboe M.** 2014. Antagonistic coevolution of marine planktonic viruses and their hosts. Ann Rev Mar Sci **6:**393–414. http://dx.doi.org/10.1146/annurev-marine-010213-135108.
34. **Koskella B, Brockhurst MA.** 2014. Bacteria–phage coevolution as a driver of ecological and evolutionary processes in microbial communities. FEMS Microbiol Rev **38:**916–931. http://dx.doi.org/10.1111/1574-6976.12072.
35. **O'Loughlin CT, Miller LC, Siryaporn A, Drescher K, Semmelhack MF, Bassler BL.** 2013. A quorum-sensing inhibitor blocks *Pseudomonas aeruginosa* virulence and biofilm formation. Proc Natl Acad Sci U S A **110:**17981–17986. http://dx.doi.org/10.1073/pnas.1316981110.
36. **Pei R, Lamas-Samanamud GR.** 2014. Inhibition of biofilm formation by T7 bacteriophages producing quorum-quenching enzymes. Appl Environ Microbiol **80:**5340–5348. http://dx.doi.org/10.1128/AEM.01434-14.
37. **Silva-Rubio A, Avendaño-Herrera R, Jaureguiberry B, Toranzo AE, Magariños B.** 2008. First description of serotype O3 in *Vibrio anguillarum* strains isolated from salmonids in Chile. J Fish Dis **31:**235–239. http://dx.doi.org/10.1111/j.1365-2761.2007.00878.x.
38. **Matsuzaki S, Tanaka S, Koga T, Kawata T.** 1992. A broad-host-range vibriophage, KVP40, isolated from sea water. Microbiol Immunol **36:**93–97. http://dx.doi.org/10.1111/j.1348-0421.1992.tb01645.x.
39. **Milton DL, O'Toole R, Horstedt P, Wolf-Watz H.** 1996. Flagellin A is essential for the virulence of *Vibrio anguillarum*. J Bacteriol **178:**1310–1319.
40. **Ghosh D, Roy K, Williamson KE, Srinivasiah S, Wommack KE, Radosevich M.** 2009. Acyl-homoserine lactones can induce virus production in lysogenic bacteria: an alternative paradigm for prophage induction. Appl Environ Microbiol **75:**7142–7152. http://dx.doi.org/10.1128/AEM.00950-09.
41. **Adams MH.** 1959. Bacteriophages. Interscience Publishers, New York, NY.
42. **Hosseinidoust Z, Tufenkji N, van de Ven TG.** 2013. Formation of biofilms under phage predation: considerations concerning a biofilm increase. Biofouling **29:**457–468. http://dx.doi.org/10.1080/08927014.2013.779370.
43. **O'Toole GA, Pratt LA, Watnick PI, Newman DK, Weaver VB, Kolter R.** 1999. Genetic approaches to study of biofilms. Methods Enzymol **310:**91–109.
44. **Wang S-Y, Lauritz J, Jass J, Milton DL.** 2003. Role for the major outer-membrane protein from *Vibrio anguillarum* in bile resistance and biofilm formation. Microbiology **149:**1061–1071. http://dx.doi.org/10.1099/mic.0.26032-0.
45. **Burmølle M, Hansen LH, Oregaard G, Sørensen SJ.** 2003. Presence of *N*-acyl homoserine lactones in soil detected by a whole-cell biosensor and flow cytometry. Microb Ecol **45:**226–236. http://dx.doi.org/10.1007/s00248-002-2028-6.
46. **Svenningsen SL, Waters CM, Bassler BL.** 2008. A negative feedback loop involving small RNAs accelerates *Vibrio cholerae*'s transition out of quorum-sensing mode. Genes Dev **22:**226–238. http://dx.doi.org/10.1101/gad.1629908.
47. **Crisafi F, Denaro R, Genovese M, Yakimov M, Genovese L.** 2014. Application of relative real-time PCR to detect differential expression of virulence genes in *Vibrio anguillarum* under standard and stressed growth conditions. J Fish Dis **37:**629–640. http://dx.doi.org/10.1111/jfd.12158.
48. **Schmittgen TD, Livak KJ.** 2008. Analyzing real-time PCR data by the comparative C_T method. Nat Protoc **3:**1101–1108. http://dx.doi.org/10.1038/nprot.2008.73.